Int. J. Electrochem. Sci., 10 **(2015)** 140 - 150

International Journal of
ELECTROCHEMICAL
SCIENCE
www.electrochemsci.org

Superconducting Fluctuations and Excess Conductivity Analysis of Re Substituted $(Tl_{1-x}Re_x)Sr_2CaCu_2O_{7-\delta}$

Annas Al-Sharabi[1,2], *R. Abd-Shukor*[1,*]

[1]School of Applied Physics, Universiti Kebangsaan Malaysia, 43600 Bangi, Selangor, Malaysia
[2] Department of Physics, Faculty of Applied Sciences, Thamar University, Thamar, Republic of Yemen
[*]E-mail: ras@ukm.my

Received: 9 September 2014 / *Accepted:* 20 October 2014 / *Published:* 17 November 2014

Samples with nominal starting compositions $(Tl_{1-x}Re_x)Sr_2CaCu_2O_{7-\delta}$ (x = 0.05- 0.30) were prepared by the solid state reaction method. Superconducting fluctuations and excess conductivity analysis was carried out using the Aslamazov-Larkin (AL) theory to determine the dimension of fluctuation induced conductivity λ. The Lawrence-Donaich (LD) theory was used to calculate the coherence length $\xi_c(0)$, Josephson coupling J, and anisotropy $\gamma = (\xi_{ab}(0)/\xi_c(0))$. XRD patterns indicated that the samples were dominantly Tl-1212 phase. Substitution of Re in place of Tl in $(Tl_{1-x}Re_x)Sr_2CaCu_2O_{7-\delta}$ showed $T_{c\ onset}$ between 70 K (x = 0.05) and 82 K (x = 0.25). Excess conductivity analyses showed that Re substitution induced 2D-to-3D conductivity transition with the highest transition temperature, T_{2D-3D} observed at x = 0.25. The calculations based on Lawrence-Doniach model showed the shortest coherence length, $\xi_c(0)$ and highest anisotropy(γ =13.42) for the x = 0.25 sample.

Keywords: Tl-1212; solid state reaction; excess conductivity; rhenium

1. INTRODUCTION

The $TlSr_2CaCu_2O_{7-\delta}$ superconductor was reported to be superconducting with T_c around 70–80 K [1]. However, the Tl-1212 superconducting phase is not easy to prepare in pure form because of the high formal Cu valence (2.5+) and overdoping of hole carriers [2]. Substitution with elements of higher valence can reduce the formal valence of Cu to the optimal value of around 2.25+ to 2.3+, improves the superconducting properties and stabilizes the Tl-1212 phase [1-4]. Reduction of the overdoped hole carrier concentrations to the optimal value results in the stabilization of the Tl-1212 phase. Partial substitution of Bi, Pb or Cr can stabilize the Tl-1212 superconducting phase [5-8].

Superconducting fluctuations behaviour (SFB) greatly affects the superconducting properties.. This includes the electrical resistivity that deviates from the liner metallic normal state behaviour well above the zero-resistance-temperature, $T_{c\ zero}$. Superconducting fluctuation behaviour dominates the excess conductivity region which arises from the Cooper pairs that start to form at the very initial stage [9]. Fluctuation induced conductivity behaviour provides the dimensionality of the superconducting fluctuation and coherence length at its critical region [10].

High temperature superconductors (HTSCs) including Tl-1212 exhibit normal and superconducting-state which are highly anisotropic which results in fluctuation of the order parameter due to the short coherence lengths along the *c*-axis, $\xi_c(0)$. The linear resistivity vs. temperature curve bends down above T_c due to the enhanced conductivity which is attributed to superconducting fluctuations [11]. These fluctuations can be analyzed by using the Aslamazov-Larkin (AL) and Lawrence-Doniach (LD) model. Subtracting the background normal state conductivity from the measured conductivity gives the excess conductivity [12]:

$$\Delta\sigma = 1/\rho_{\ measured} - 1/\rho_{\ background} \qquad (1)$$

where ρ is the resistivity. Excess conductivity can be written as [13]:

$$\Delta\sigma/\sigma_o = A\ \varepsilon^{-\lambda} \qquad (2)$$

where σ_o is the conductivity at 300 K, ε is the reduced temperature given by the relation [14].

$$\varepsilon = \ln (T/ T^p_c) / T^p_c = (T - T^p_c) / T^p_c \qquad (3)$$

where T^p_c is the temperature of the peak obtained from $d\rho/dT$. *A* is the AL temperature independent constant and λ is the critical exponent which is related to the conduction dimensionality D where $\lambda = 2 - D/2$. For the 1-dimensional region (1D), $\lambda = 1.5$, for 2-dimensional region (2D), $\lambda = 1.0$, and for 3D, $\lambda = 0.5$. λ can be obtained from the slope of $\ln(\Delta\sigma/\sigma_o)$ versus $\ln(\varepsilon)$ plot. Interestingly, elemental substitutions also contribute to the changes in T_{2D-3D} and coherence length [15]. For Tl-1212, this enhancement leads to a longer $\xi_c(0)$ and enhanced the superconducting properties due to the reduction in the anisotropy, γ and increase in the interlayer coupling, *J* [15].

At the transition temperature, T_{2D-3D}, the coherence length along *c*-axis, $\xi_c(0)$ for polycrystalline samples can be obtained by using the Lawrence-Doniach model [14]:

$$T_{2D-3D} = T_c\ [1 + (2\ \xi_c(0)\ /d)^2] \qquad (4)$$

where *d* is the distance between the superconducting layers. For Tl-1212, *d* = 3.18 Å [14]. Using the Lawrence-Doniach model, the concept of interlayer coupling, *J* based on Josephson coupling as a result of $\xi_c(0)$ interaction with the superconducting layers is given by [16]:

$$J = [2\ \xi_c(0)\ ]^2 /d^2 \qquad (5)$$

For layered superconducting systems the anisotropy γ is expressed by [17]:

$$\gamma = \xi_{ab}(0)\ /\ \xi_c(0) \qquad (6)$$

where $\xi_{ab}(0)$ is the *ab*-coherence length which is between 10 and 20 Å for copper oxide-based HTSC [14].

There has been report on the effect of Cr on the superconductivity and formation of the Tl-1212 phase [18]. The (Cu, Tl)-based [19-22] revealed a cross over from 2D to 3D fluctuation behaviour with decreasing temperature. $Tl_{1-x}Cu_xSr_{1.2}Yb_{0.8}CaCu_2O_{7-d}$ [23] and $Tl_{0.5}Pb_{0.5}Sr_{2-x}Yb_xCaCu_2O_{7-d}$ [19] show strong influence of substitutions on the fluctuation behaviour with transition from 2D to 3D

behaviour. $Tl_{0.8}Hg_{0.2}Ba_2$ $Ca_{2-x}R_xCu_3O_{9-d}$ (R = Sm and Yb) shows the transitions from 1D to 2D and 2D to 3D as the temperature was lowered [24].

Substitution of multivalent ions such as chromium ($Cr^{3+}/Cr^{5+}/Cr^{7+}$) results in a higher T_c than ion with only one valence such as most of rare-earth elements. Re is another element with multivalent ion ($Re^{4+}/Re^{5+}/Re^{6+}/Re^{7+}$). It is interesting to investigate the effect of multivalent rhenium (ionic radius $\leq$ 0.063 nm) at the Tl site (with Tl^{3+} ionic radius 0.095 nm).

In this paper, we report the effect of Re substitution at the Tl site in $(Tl_{1-x}Re_x)Sr_2CaCu_2O_{7-\delta}$ (x = 0.05, 0.10, 0.15, 0.20, 0.25 and 0.30) superconductors. Results of electrical resistivity (dc) measurements and powder X-ray diffraction are presented. The chemical composition of the samples was determined using energy dispersive X-ray analysis (EDX). The Aslamazov-Larkin (AL) theory was employed to determine the dimension of fluctuation induced conductivity, λ. The Lawrence-Donaich (LD) theory was used to calculate $\xi_c(0)$, J and γ of the superconducting samples.

2. EXPERIMENTAL DETAILS

Samples with nominal starting composition $(Tl_{1-x}Re_x)Sr_2CaCu_2O_{7-\delta}$ (x = 0.05, 0.10, 0.15, 0.20, 0.25 and 0.30) were prepared using the solid-state reaction method. High purity ($\geq$ 99.99 %) SrO, CaO and CuO were mixed in the appropriate amounts and ground before being calcined at 900 ºC for over 48 h with several intermittent grindings to obtain a uniform black powder. Then appropriate amounts of Tl_2O_3 and ReO_2 were added to the precursor and completely mixed. The powders were then pressed into pellets with diameter 13 mm and thickness of around 2 mm. In order to compensate for the thallium loss during heating, excess 10 % Tl_2O_3 was added. The pellets were heated at 1000 ºC for 4 min in flowing O_2 followed by furnace cooling.

The dc electrical resistance were measured using the four point probe method. Silver paste was used as electrical contact. A CTI Cryogenics Closed Cycle Refrigerator Model 22 and Lake Shore Temperature Controller Model 340 were used for low temperature measurements. The powder X-ray diffraction method was used to determine the resultant phases. A Bruker model D8 Advance diffractometer with CuKα source was used. The lattice parameters were calculated by employing at least 15 diffraction peaks. The 1212:1201 volume fractions were calculated from the diffraction intensities of 1212 and 1201 using the equations [14]:

$$\mathrm{Tl}-1212(\%) = \frac{\sum I_{1212}}{\sum I_{1212} + \sum I_{1201}} \times 100\% \qquad (5)$$

$$\mathrm{Tl}-1201(\%) = \frac{\sum I_{1201}}{\sum I_{1212} + \sum I_{1201}} \times 100\% \qquad (6)$$

where I is the peak intensity of the phase. Energy dispersive X-ray analysis (EDX) was used to determine the resultant chemical composition.

3. RESULTS AND DISCUSSION

X-ray powder diffraction patterns for $(Tl_{1-x}Re_x)Sr_2CaCu_2O_{7-\delta}$ (x = 0.05, 0.10, 0.15, 0.20, 0.25 and 0.30) are shown in Figure 1. The patterns indicated that the Tl-1212 phase with tetragonal unit

cell (space group, P4/mmm) was dominant with a few weak diffraction lines of Tl-1201, and an unknown phase.

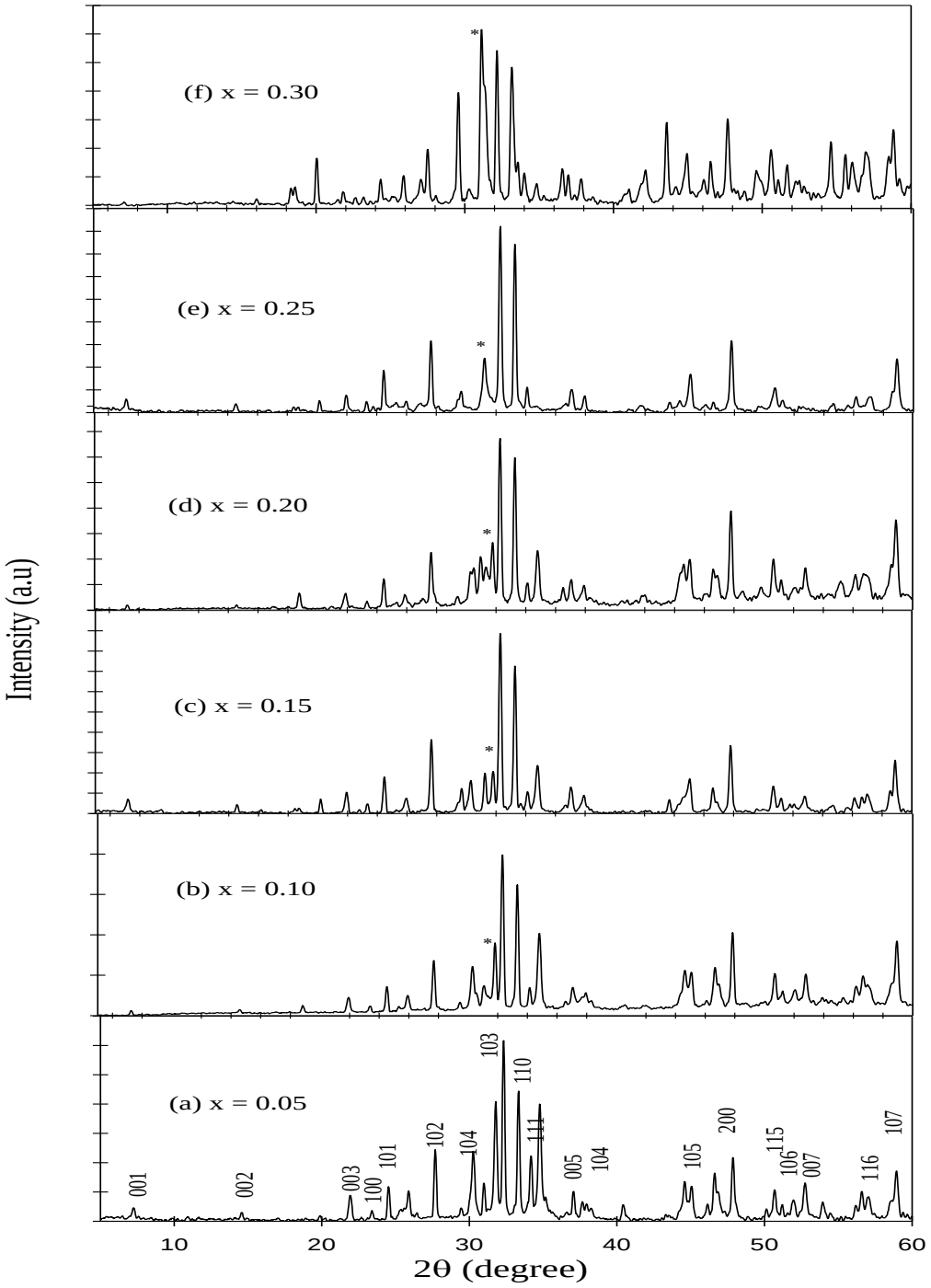

Figure 1. Powder X-ray diffraction patterns for $(Tl_{1-x}Re_x)Sr_2CaCu_2O_{7-\delta}$ (x = 0.05, 0.10, 0.15, 0.20, 0.25 and 0.30) samples showing major 1212 phase. The 1201 phase is indicated by (*)

The x = 0.25 showed the highest Tl-1212 volume fraction (88%). This may due to the effect of the ionic radii of the elements involved and certain values are preferred. When the amount of the smaller Re ions (with radii equal to or less than 0.063 nm) was increased and the larger Tl+3 was

decreased (0.095 nm), the average radius decreased and became too small to participate in the formation of 1212 phase. $T_{c\ onset}$, $T_{c\ zero}$, resistivity (at 297 K), 1212:1201 volume fraction and 1212 lattice parameters for $(Tl_{1-x}Re_x)Sr_2CaCu_2O_{7-\delta}$ are shown in Table 1.

Table 1. $T_{c\ onset}$, $T_{c\ zero}$, 1212:1201 volume fraction, lattice parameters, T^p_c, room temperature resistivity (ρ_{297}), α , β, $T_{2D\text{-}3D}$, λ_{2D}, λ_{3D}, $\xi_c(0)$, J and γ for $(Tl_{1-x}Re_x)Sr_2CaCu_2O_{7-\delta}$ (x = 0.05, 0.10, 0.15, 0.20, 0.25 and 0.30) samples

Re (x)	0.05	0.10	0.15	0.20	0.25	0.30
$T_{c\ onset}$ (K)	70	74	77	80	82	79
$T_{c\ zero}$ (K)	59	62	65	67	72	69
1212:1201 volume fraction (vol. %)	79:21	83:17	85:15	86:14	88:12	75:25
Tl1212 lattice parameter						
a (Å) ± 0.003	3.778	3.781	3.774	3.766	3.780	3.762
c (Å) ± 0.005	12.091	12.072	12.098	12.086	12.092	12.073
T^p_c (K)	65	67	68	71	75	71
ρ_{297} (mΩcm)	0.712	0.822	2.399	2.425	3.290	4.749
$\alpha = \rho_n(0K)$(mΩcm)	0.13	0.25	0.40	0.45	0.55	0.85
$\beta = d\rho/dT \times 10^{-3}$ (mΩcm)/K	1.959	1.927	6.729	6.645	9.247	13.099
T_{2D-3D} (K)	88	92	95	98	100	97
λ_{2D}	1.027	0.945	0.879	0.875	0.891	0.867
λ_{3D}	0.518	0.515	0.492	0.505	0.513	0.479
$\xi_c(0)$ (Å)	0.806	0.784	0.769	0.754	0.745	0.759
J	0.257	0.243	0.234	0.225	0.219	0.228
γ	12.40	12.75	13.01	13.26	13.42	13.18

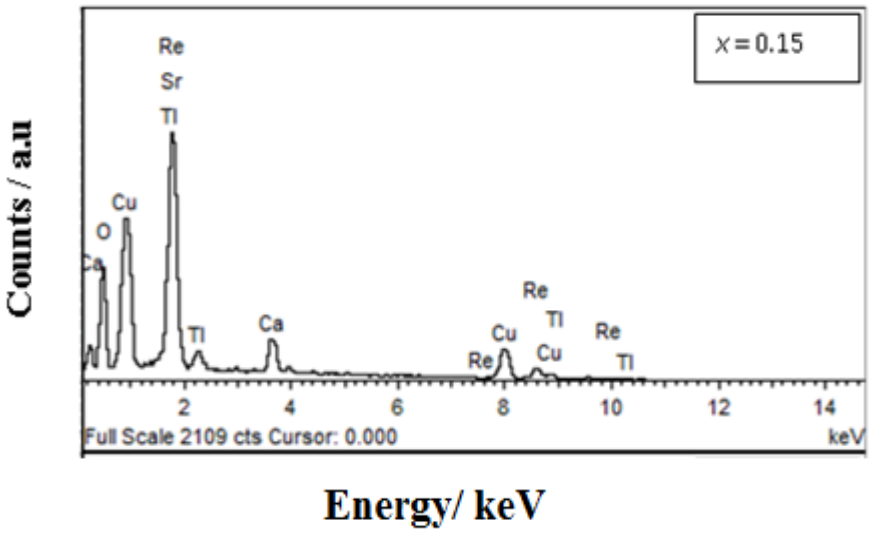

Figure 2. EDX spectrum of $(Tl_{1-x}Re_x)Sr_2CaCu_2O_{7-\delta}$ superconductor for x = 0.15

The XRD data show existence of more than one phase. One concern is that the lattice parameters of Tl1212 do not change with Re content (within the data scattering range). This could be an indication that Re does not in fact substitute into Tl1212 crystal lattice and the change of R(T) is due to impurities in the polycrystalline samples. Resistivity above T_c is strongly sensitive to inclusion of phases other than Tl1212 in the pellet sample.

Figure 2 shows the EDX spectrum of $(Tl_{1-x}Re_x)Sr_2CaCu_2O_{7-\delta}$ superconductor for x = 0.25. Table 2 shows the elemental composition of $(Tl_{1-x}Re_x)Sr_2CaCu_2O_{7-\delta}$ for x = 0.25. The energy dispersive X-ray (EDX) analysis showed the presence of elements approximately according to the Tl-1212 phase with slight modification probably due to the presence of the 1201 phase and the uncertainty in determining the oxygen content by using the EDX method.

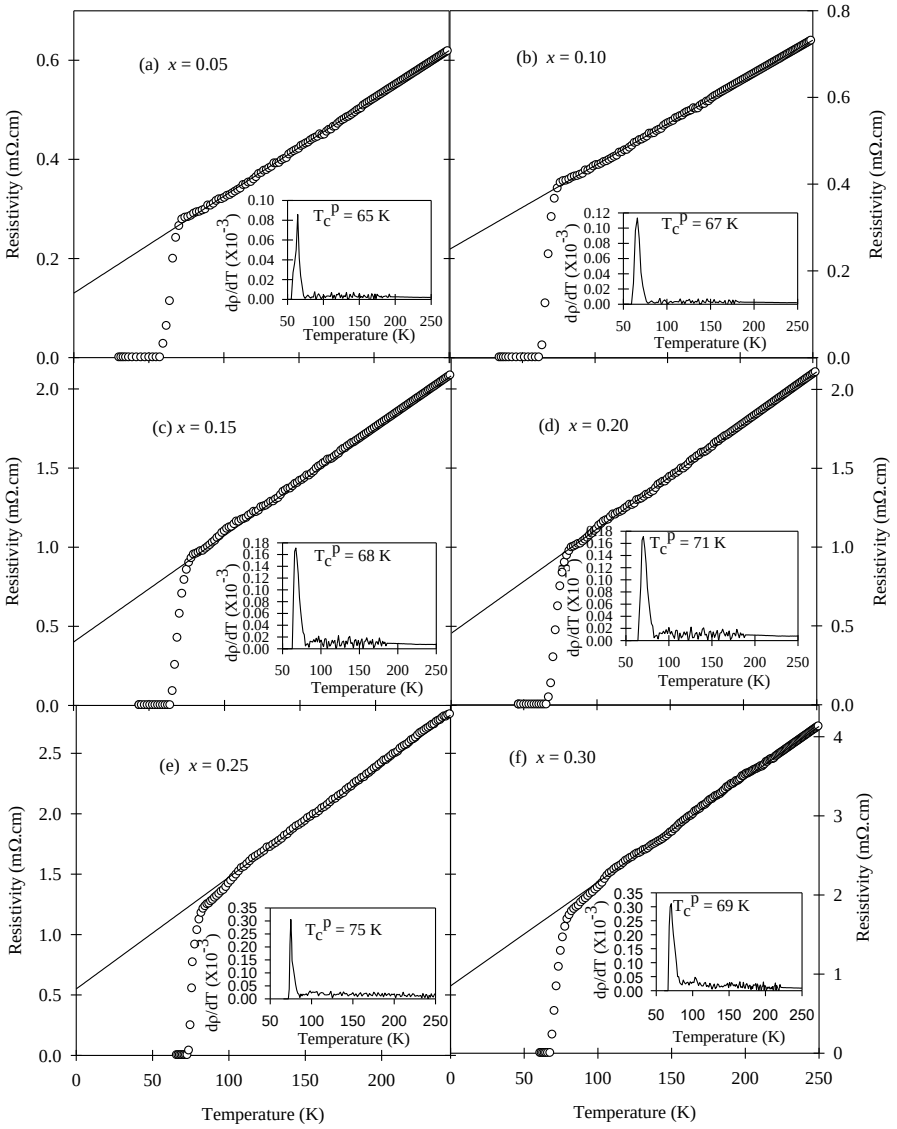

Figure 3. Electrical resistivity of $(Tl_{1-x}Re_x)Sr_2CaCu_2O_{7-\delta}$ (x = 0.05, 0.10, 0.15, 0.20, 0.25 and 0.30) samples. Inset shows plots of dρ/dT versus temperature. The linear fit curves show the background normal state resistivity projection

The normalized resistance at room temperature as a function of temperature for the $(Tl_{1-x}Re_x)Sr_2CaCu_2O_{7-\delta}$ samples for x = 0.05, 0.10, 0.15 0.20, 0.25 and 0.30 sintered at 1000 °C for 4 min is shown in Figure 3. All samples displayed metallic normal-state behaviour above $T_{c\ onset}$ followed by the superconducting transition as the temperature was lowered. $T_{c\ onset}$ for the samples with x = 0.05, 0.10, 0.15, 0.20, 0.25 and 0.30 were 70, 74, 77, 80, 82 and 79 K, respectively.

Table 2. Elemental quantitative analysis of $(Tl_{1-x}Re_x)Sr_2CaCu_2O_{7-\delta}$ superconductor for x = 0.15 superconductor as presented in EDX graph shown in Figure 2

Re(*x*)	Element	O K	Ca K	Cu L	Sr L	Re M	Tl M	Totals
0.15	Weight%	32.41	4.83	22.96	30.54	3.11	6.14	100
	Error%	0.89	0.21	0.18	0.14	0.26	0.76	
	Atomic%	69.70	4.15	12.50	12.02	0.60	1.04	

This can be explained by the hole-filling mechanism, due to partial replacement of Tl^{3+} with higher valence Re ions. The parabolic shape of T_c vs. x (Figure 4) is a typical characteristic of high-temperature superconductors substituted with higher valence ions. The addition of Re reduces holes concentration (by hole filling mechanism) which optimized the hole concentration closer to the optimal value resulting in the highest T_c at x = 0.25. Based on the observed $T_{c\ onset}$ values of between 70 and 82 K for $(Tl_{1-x}Re_x)Sr_2CaCu_2O_{7-\delta}$ (x = 0.05–0.30) it is suggested that the superconductivity is dominated by 1212 phase. T_c is related directly to the Tl-1212 vol% (Table 1), but was mostly influenced by the doping level which is related to the average copper valence. The 1201 phase has been previously reported with $T_{c\ onset}$ below 50 K.

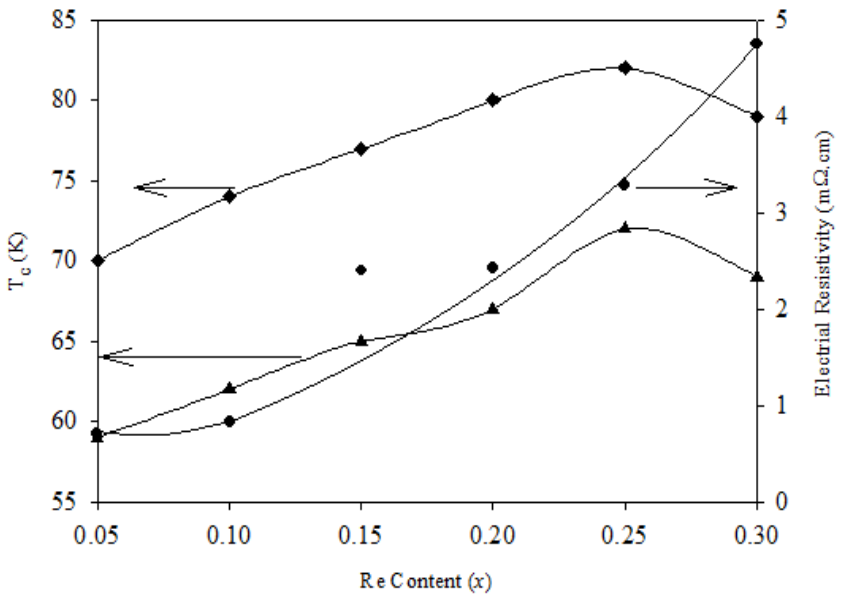

Figure 4. Normal state electrical resistivity (●) at 297 K and the variation of $T_{c\ onset}$t (♦) and $T_{c\ zero}$ (▲) as a function of x for $(Tl_{1-x}Re_x)Sr_2CaCu_2O_{7-\delta}$

The normal state electrical resistance increased with increased of Re content (Table 1). Figure 4 shows $T_{c\ onset}$, $T_{c\ zero}$ and electrical resistivity (at 297 K) as a function of *x*. The resistivity values indicate variation in the hole carrier concentration of $(Tl_{1-x}Re_x)Sr_2CaCu_2O_{7-\delta}$ (x = 0.05–0.30) with increasing Re substitution. The normal state electrical resistance increased with increased of Re content case due to electron doping and substitution of the higher valence Re^{5+} reduced average copper valence in the CuO_2 planes and caused hole concentration to decrease (Re reduces holes concentration by hole filling mechanism).

The possible valences of the metallic ions in $(Tl_{1-x}Re_x)Sr_2CaCu_2O_{7-\delta}$ are Tl^{1+}/Tl^{3+}, Sr^{2+}, Ca^{2+}, Cu^{2+}/Cu^{3+}, and $Re^{4+}/Re^{5+}/Re^{6+}/Re^{7+}$. The optimal Cu valence to maximize T_c in the Tl-1212 phase is 2.25+. By assuming that Tl is in the Tl^{3+} state and by using the optimal Cu valence (2.25+) and the fact that the x = 0.25 sample exhibited the highest T_c, the average Re valence for optimal superconductivity is 5+ (Re^{5+}). The substitution of pentavalent Re^{5+} for trivalent Tl^{+3} may have contributed to the stabilization of the 1212 phase (Table 1).

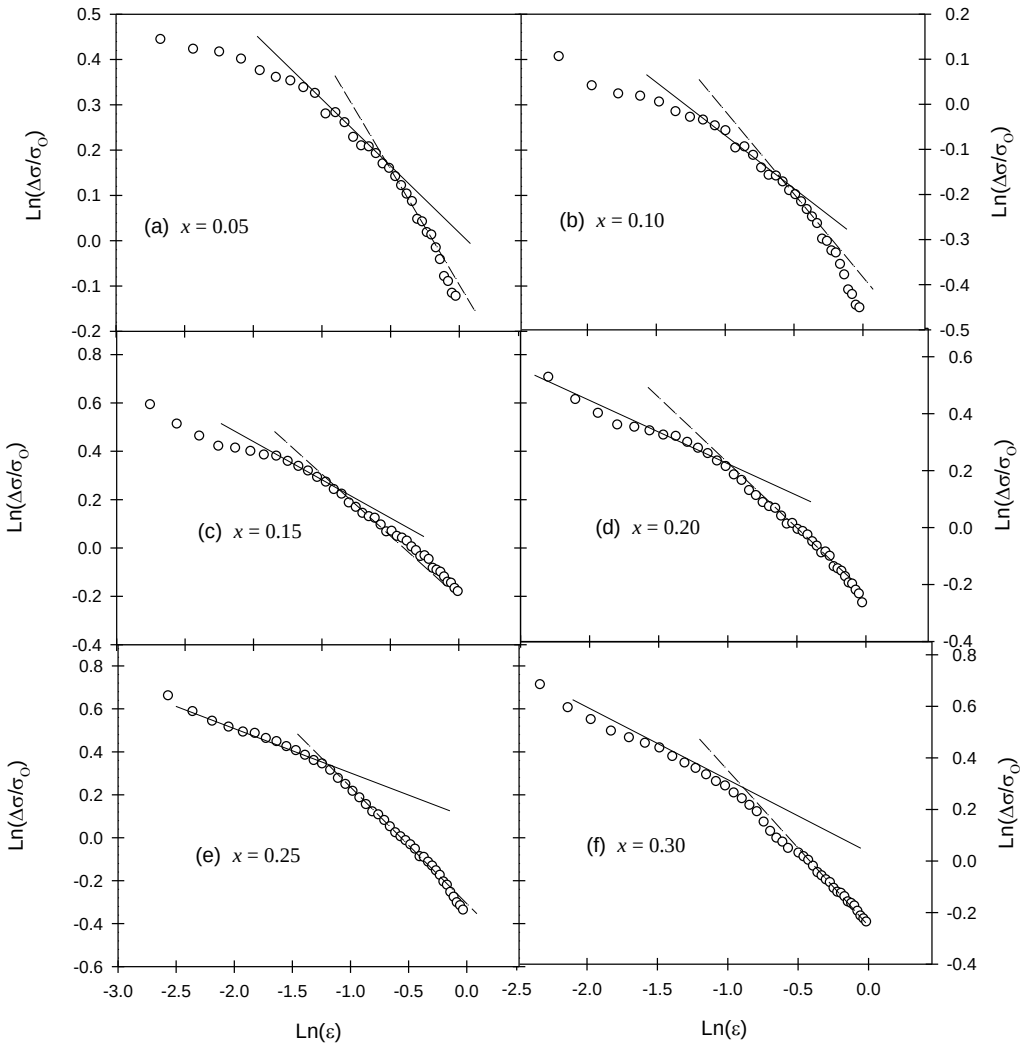

Figure 5. Plot of $ln(\Delta\sigma/\sigma o)$ versus $ln(\varepsilon)$ of $(Tl_{1-x}Re_x)Sr_2CaCu_2O_{7-\delta}$ (x = 0.05, 0.10, 0.15, 0.20, 0.25 and 0.30) samples. The solid line represents the 2-D and dotted line 3-D theoretical slope

The normal state electrical resistivity was fitted to $\rho = \alpha + \beta T$ for $x = 0.05–0.30$ (Figures 3), where α is the intercept and β is the slope of the fitted resistivity data [13]. The linear fits for the data at high temperatures are shown as straight lines. The deviation from linear behavior decreases with the resistivity because excess conductivity reveals the region where Cooper pair formation begins. The insets in Figures 3 show the temperature dependence curves for the derivative of the resistivity; the peak temperature (T^p_c) was used to calculate the reduced temperature (ε). All samples showed almost a single peak at T_c, indicating a superconducting transition within the grains. The values of various parameters such as T^p_c, the room temperature resistivity (ρ_{297}), α and β are listed in Table 1 for all samples.

The deviation of resistivity, $\rho(T)$ from the background linear resistivity revealed excess conductivity (Δσ). To compare the experimental data with the theoretical expression for fluctuation conductivity, a graph of $ln(\Delta\sigma/\sigma_o)$ versus $ln(\varepsilon)$ was plotted (Figures 5). This figure shows the fluctuation conductivity for all samples covering the mean field regime: $-3 < ln(\varepsilon) < 1$. Table 1 shows the calculated values for $T_{2D\text{-}3D}$, $\xi_c(0)$, J and γ for the $(Tl_{1-x}Re_x)Sr_2CaCu_2O_{7-\delta}$ samples. It is clear that each plot showed two significant different regions. In order to compare the experimental data with theoretical predictions, the different regions of the plots are linearly fitted and the conductivity exponent λ values are determined from the slopes and listed in Table 1. Fluctuation phenomena in the superconducting cuprates would have a significant effect on our understanding of the superconducting process in these materials. With further decreasing in temperature a crossover between two dimensional fluctuations and three dimensional is observed at temperature above T_c. The mean field region, for each sample, consists of two distinct linear parts. For the first part, at higher temperature, the conductivity exponent values λ_{2D} vary from -1.027 to -0.867, indicating the existence of 2D fluctuations. Whilst at lower temperature, the conductivity exponent values λ_{3D} vary from -0.518 to -0.479 reflecting the appearance of 3D fluctuations. The 3D-2D crossover temperatures $T_{3D\text{-}2D}$ are calculated from the intersection of the two linear parts and the values are listed in Table 1. The shortest $\xi_c(0)$ within the series was 0. 745 Å at $x = 0.25$. This sample also showed the lowest J value (0.219) and the highest anisotropy (γ) (13.42). Therefore, Re substitution modified $\xi_c(0)$, consequently increased the anisotropy of the samples and reduced the interlayer coupling strength. This reduction however does not suppress the transition temperature. It is clear that the shortest coherence length along the *c*-axis lies in the optimum-doped region. However the coherence length drops in the under-doped region and increases in the over-doped side with the increase of hole concentration. All the values of inter-layer coupling J are less than one, indicating a weak coupling between the CuO_2-planes. Also, J decreases as the substitution-content increases. This means that, the partial replacement of Tl^{+3} ions by either Re^{+5} ions weakens the CuO_2 interlayer coupling in the $(Tl_{1-x}Re_x)Sr_2CaCu_2O_{7-\delta}$ samples. Excess conductivity analysis was also recently reported for $TlSr_2(Ca_{1-x}Re_x)Cu_2O_{7-\delta}$ [25]. It was found that Re substitution decreased $\xi_c(0)$ with increased of x [25]. Moreover, Re substitution caused changes in $T_{2D–3D}$; the highest transition was observed at $x = 0.15$ [25]. Excess conductivity analyses of $Tl_{0.9}Bi_{0.1}Sr_{1.8}Yb_{0.2}Ca_{1-x}Cd_xCu_{1.99}Fe_{0.01}O_{7-\delta}$ [11] showed that Cd substitution influenced $T_{2D–3D}$, $\xi_c(0)$ and J. Interestingly, changes in $\xi_c(0)$ due to elemental substitution was also previously reported for other Tl-1212 compound [14,15], $Tl_{0.5}Pb_{0.5}Sr_{2-x}Yb_xCaCu_2O_{7-\delta}$ [19] and $Tl_{1-x}Cu_xSr_{1.2}Yb_{0.8}CaCu_2O_{7-\delta}$ [23].

For $(Tl_{1-x}Re_x)Sr_2CaCu_2O_{7-\delta}$, the x = 0.25 sample showed the highest T_c and the highest 1212 phase. The decrease in coherence length along the *c*-axis promotes an increase in anisotropy (γ), possibly explaining the superconducting behavior when $T_{c\ onset}$ exceeds 70 K. The deviation of linearity in R(T) is the strongest for the sample with highest nominal Re content. This would imply that these deviations are indeed due to impurities in the pellets, containing Re.

The average slope β increased from 1.959×10^{-3} to 13.099×10^{-3} (mΩ-cm)/K as x increased from 0.05 to 0.30 due to the change in carrier concentration when Re-content increased. Excess conductivity analyses for $(Tl_{1-x}Re_x)Sr_2CaCu_2O_{7-\delta}$ indicated that 2D- to 3D transitions in the normal state were induced by the partial substitution of Re into the Tl sites. Excess conductivity analyses of $TlSr_2(Ca_{1-x}Re_x)Cu_2O_{7-\delta}$ which showed 2D fluctuation behavior [25] is similar to that of the Re substituted samples in this work (Figure 5) and also from previous reports on (Cu, Tl)-based [20-22], Cu-substituted $Tl_{1-x}Cu_xSr_{1.2}Yb_{0.8}CaCu_2O_{7-\delta}$, $Tl_{1-x}Cu_xSr_{1.6}Yb_{0.4}CaCu_2O_{7-\delta}$ [15, 23] and Yb-substituted $Tl_{0.5}Pb_{0.5}Sr_{2-x}Yb_xCaCu_2O_{7-\delta}$ [19] superconductors which showed 2D to 3D transition behaviors. The calculated $\xi_c(0)$ values were comparable to those (0.03–0.68 nm) reported for double-layered Tl-based compounds. The small $\xi_c(0)$ values indicated the high degree of anisotropy in the Tl-1212 samples. Excess conductivity analyses revealed the dependence of $\xi_c(0)$ on the amount of Re substitution in the $(Tl_{1-x}Re_x)Sr_2CaCu_2O_{7-\delta}$. Moreover, Re substitution caused changes in T_{2D-3D}; the highest transition was observed at x = 0.25. Our calculations showed a decrease in J with Re (x = 0.05 to 0.25) substitution.

5. CONCLUSION

This work showed that ReO_2 was effective for the formation of the Tl-1212 phase. Excess conductivity analyses of $(Tl_{1-x}Re_x)Sr_2CaCu_2O_{7-\delta}$ indicated that 2D to 3D transition in the normal state can be induced by partial substitution of Re for Tl. The x = 0.25 sample showed the lowest value of $\xi_c(0)$ (0.745 Å) which also recorded the highest anisotropy, γ (13.42). These results indicate that Re substitution modified $\xi_c(0)$ and consequently decreased the interlayer coupling strength and increased the anisotropy of the samples. Moreover, Re substitution caused changes in T_{2D-3D} with the highest transition observed at x = 0.25. The decrease in inter-layers coupling as a result of Re substitution may be the reason for variation in $T_{c\ zero}$. A strong correlation between $T_{c\ onset}$ and T_{2D-3D} was observed in these superconductors.

ACKNOWLEDGEMENTS
This work has been supported by the Ministry of Education of Malaysia under grant no.: FRGS/2/2013/SG02/UKM/01/1 and Universiti Kebangsaan Malaysia under grant no: UKM-DIP-2012-032.

References

1. C. Martin, J. Provost, D. Bourgault, D. Domenses, C. Michel, M. Herviu and B. Raveau, *Physica C*. 157 (3) (1989) 460-468.

2. M.A. Subramanian, C.C. Torardi, J. Gopalakrishnan, P.L. Gai, J.C. Calabrese, T.R. Askew, R.B. Flippen and A.W. Sleight, *Science*. 242 (1988) 249-252.
3. Z. Y. Chen, Z. Z. Sheng, Y.Q. Tang, Y. F. Li and D. O. Pederson, *Solid State Communication*. 83 (11) (1992) 895-898.
4. Z. Z. Sheng, Y. F. Li and D. O. Pederson, *Solid State Communication*. 80 (11) (1991) 913-915.
5. S. Li and M. Greenblatt, *Physica C*. 157 (2) (1989) 365-369.
6. R. Abd-Shukor and K. S. Tee, *Materials Science Letters.* 17 (2) (1997) 103-106.
7. Y. F. Li, O. Chmaissem and Z. Z. Sheng, *Physica C*. 248 (1-2) (1995) 42-48.
8. A. Al-Sharabi and R. Abd-Shukor, *International Journal of Electrochemical Science*. 8 (2013) 7825 – 7830.
9. M. Cardona, *Physica C*. 317–318 (1999) 30-54.
10. M.R. Islam and M.H.A. Pramanik, *Physical review B*. 55 (10) (1997) 6621-6624.
11. S. Ismail, A.K. Yahya and N.A. Khan, *Ceramics International*. 39 (2013) S257–S261.
12. S.V. Sharma, G. Sinha, T.K. Nath, S. Chakroborty and A.K. Majumdar, *Physica C*. 242 (1995) 351-359.
13. T. Sato, H. Nakane, N. Mori and S. Yoshizawa, *Physica C*. 357–360 (2001) 244-147.
14. A. Ali Yusuf, A.K. Yahya, N.A. Khan, F. Md. Salleh, E. Marsom and N. Huda, *Physica C*. 471 (11-12) (2011) 363-372.
15. N.H. Ahmad, N.A. Khan and A.K. Yahya, *Journal of Alloys and Compounds*. 492 (1-2) (2010) 473-481.
16. N. A. Khan and A. Mumtaz, *Physica B*. 404 (13) (2010) 2772-2780.
17. N.A. Khan, N. Hassan, M. Irfan and T. Firdous, *Physica B*. 405 (6) (2010) 1541-1545.
18. Z. Z. Sheng, D. X. Gu, Y. Xin and D. O. Pederson, *Modern Physics Letters B*. 9 (1991) 635-642.
19. N. Huda, A.K. Yahya and W.F. Abdullah, *American Institute of Physics (AIP) Proceedings, American Institute of Physics*. 1017 (2008) 114-118.
20. N.A Khan and M. Irfan, *Physica C*. 468 (2008) 2341-2344.
21. N.A. Khan and G. Husnain, *Physica C*. 436 (1) (2006) 51-58.
22. N.A. Khan, A.A. Khurram and A. Maqsood, *Physica C*. 398 (3-4) (2003) 114-122.
23. N. Huda and A.K. Yahya, *Materials Research Innovation*. 13(3) (2009) 406.
24. R. Awad, A.I. Abou-Aly, I.H. Ibrahim and W. Abddeen, *Solid State Communications.* 146(1) (2008) 92-96.
25. A. Al-Sharabi and R. Abd-Shukor, *Ceramics International*. 40 (2014) 9383–9388.

© 2015 The Authors. Published by ESG (www.electrochemsci.org). This article is an open access article distributed under the terms and conditions of the Creative Commons Attribution license (http://creativecommons.org/licenses/by/4.0/).